Proc. Natl. Acad. Sci. USA
Vol. 92, pp. 2479–2483, March 1995
Immunology

Crystal structure of an H-2K^b–ovalbumin peptide complex reveals the interplay of primary and secondary anchor positions in the major histocompatibility complex binding groove

(murine major histocompatibility complex class I/allele-specific motifs/x-ray crystallography)

DAVED H. FREMONT*†‡, ENRICO A. STURA*, MASAZUMI MATSUMURA§¶, PER A. PETERSON§‖, AND IAN A. WILSON*,**

Departments of *Molecular Biology and §Immunology, The Scripps Research Institute, La Jolla, CA 92037; and †Department of Chemistry, University of California, San Diego, La Jolla, CA 92093

Communicated by John W. Kappler, National Jewish Center for Immunology and Respiratory Medicine, Denver, CO, November 30, 1994

ABSTRACT **Sequence analysis of peptides naturally presented by major histocompatibility complex (MHC) class I molecules has revealed allele-specific motifs in which the peptide length and the residues observed at certain positions are restricted. Nevertheless, peptides containing the standard motif often fail to bind with high affinity or form physiologically stable complexes. Here we present the crystal structure of a well-characterized antigenic peptide from ovalbumin [OVA-8, ovalbumin-(257–264), SIINFEKL] in complex with the murine MHC class I H-2K^b molecule at 2.5-Å resolution. Hydrophobic peptide residues Ile-P2 and Phe-P5 are packed closely together into binding pockets B and C, suggesting that the interplay of peptide anchor (P5) and secondary anchor (P2) residues can couple the preferred sequences at these positions. Comparison with the crystal structures of H-2K^b in complex with peptides VSV-8 (RGYVYQGL) and SEV-9 (FAPGNYPAL), where a Tyr residue is used as the C pocket anchor, reveals that the conserved water molecule that binds into the B pocket and mediates hydrogen bonding from the buried anchor hydroxyl group could not be likewise positioned if the P2 side chain were of significant size. Based on this structural evidence, H-2K^b has at least two submotifs: one with Tyr at P5 (or P6 for nonamer peptides) and a small residue at P2 (i.e., Ala or Gly) and another with Phe at P5 and a medium-sized hydrophobic residue at P2 (i.e., Ile). Deciphering of these secondary submotifs from both crystallographic and immunological studies of MHC peptide binding should increase the accuracy of T-cell epitope prediction.**

Class I major histocompatibility complex (MHC) molecules bind short peptide fragments of intracellularly processed proteins and display them for surveillance by cytotoxic T cells (1). Peptides presented by class I molecules are characterized by allele-specific motifs (2), in that pooled sequencing studies of naturally presented peptides have shown them to be of restricted length (typically 8 or 9 amino acids) and to contain specific anchor residues. X-ray crystal structures of single peptide complexes of MHC class I molecules (3–7) indicate that the anchor residues bind in the deep pockets of the binding groove that are formed by polymorphic residues. Although these anchor residues are usually necessary for high-affinity binding and stabilization of individual MHC molecules, the anchor motif defined by pooled sequencing is not a sufficient prerequisite by itself to define the high affinity and specificity of MHC–peptide interactions (8). Peptide analog studies have clearly demonstrated the important role of secondary anchor residues in peptide binding, and indeed, substantial improvements in epitope predictions have resulted from the development of extended motifs including these additional sequence restrictions (9). In at least two cases, analysis of a large number of individual peptide sequences that bind to a particular MHC molecule has indicated the presence of submotifs (10, 11). Thus for both MHC class I and class II binding peptides, the usage of alternate auxiliary anchor residues can result in a correlated residue preference at neighboring sites in the sequence.

Pooled sequencing of naturally processed ligands of H-2K^b reveals a strong preference for octamers (P1–P8) with Tyr or Phe at P5, Leu or Met at P8, and to a lesser extent a Tyr at P3 (12). We have shown (3, 13) that the anchor residues at positions P5 and P8 of VSV-8 (RGYVYQGL) and P6 and P9 or SEV-9 (FAPGNYPAL) are deeply buried in the central and C-terminal pockets C and F of the H-2K^b binding groove, respectively. In VSV-8, Tyr-P3 acts as a secondary anchor and is located in the shallower and more surface-accessible pocket D of H-2K^b, which is significantly altered in structure in the SEV-9 complex (with Pro at P3). Neither of these peptides makes extensive use of pocket B in H-2K^b, which is contiguous with the deeply invaginated pocket C (for discussion, see ref. 13). To further our understanding of how a wide array of disparate peptide sequences can bind to the product of a specific class I allele, we have determined the x-ray crystal structure of H-2K^b bound with OVA-8, the extensively characterized immunodominant peptide of chicken ovalbumin (residues 257–264, SIINFEKL) (14).††

MATERIALS AND METHODS

Crystallization and Data Collection. The soluble extracellular domains of H-2K^b (heavy chain residues 1–274 and β_2-microglobulin residues B1–B99) were produced in *Drosophila melanogaster* cell culture and purified to homogeneity (15, 16). Crystals of the H-2K^b–OVA-8 complex were grown in 2.0 M NaH_2PO_4/K_2HPO_4 with 1% 2-methyl-2,4-pentanediol at pH 6.2 by macroseeding as described (17) but at a lower temperature of 17.0°C to produce a slower growth rate.

The publication costs of this article were defrayed in part by page charge payment. This article must therefore be hereby marked "*advertisement*" in accordance with 18 U.S.C. §1734 solely to indicate this fact.

Abbreviations: MHC, major histocompatibility complex; vdw, van der Waals.

‡Present address: Howard Hughes Medical Institute, Department of Biochemistry and Molecular Biophysics, Columbia University, New York, NY 10032; and Division of Basic Immunology, National Jewish Center for Immunology and Respiratory Medicine, Denver, CO 80206.

¶Present address: Supragen, Inc., 1670 Pierce Street, Lakewood, CO 80214.

‖Present address: R. W. Johnson Pharmaceutical Research Institute, 3535 General Atomic Court, San Diego, CA 92121.

**To whom reprint requests should be addressed.

††The atomic coordinates have been deposited in the Protein Data Bank, Chemistry Department, Brookhaven National Laboratory, Upton, NY 11973 (reference 1VAC).

Data to 2.5-Å resolution were collected from a single crystal at room temperature on a Siemens (Madison, WI) area detector mounted on an Elliott (Borehamwood, U.K.) GX-18 rotating anode x-ray generator operating at 40 kV and 55 mA. The crystals belong to monoclinic space group $C2$ with cell dimensions of a = 118.0 Å, b = 60.9 Å, c = 83.8 Å, and β = 107.6°, with a solvent content (18) of 62%, and with a single H-2K^b complex per asymmetric unit. A total of 43,371 observations were recorded to 2.5-Å resolution from a single crystal and subsequently reduced (19) to 18,598 reflections (93.6% complete between ∞ and 2.5 Å) with an $R_{sym}(I)$ = 5.9 and an average I/σ = 16.0.

Structure Determination and Refinement. Initial phases for the H-2K^b–OVA-8 complex were determined by molecular replacement using the coordinates of the 2.3-Å H-2K^b–VSV-8 complex (Protein Data Bank entry 1VAA) (20). Both rotation (21) and translation (22) functional analyses gave clear and unambiguous solutions. Model building was undertaken with the University of California, San Diego, version of FRODO (23), typically employing 30 amino acid omit maps. The current model, derived from XPLOR (24) atomic refinement using Engh and Huber parameters (25), includes 373 residues of H-2K^b (3053 nonhydrogen atoms), the OVA-8 peptide (68 nonhydrogen atoms), and 109 water molecules, which were initially identified by peak picking from F_o-F_c maps and kept only if no steric clashes resulted and the individual B values were <60 Å^2 after refinement. Electron density maps of the complex are of good to excellent quality (Fig. 1). The R value for 6.0- to 2.5-Å data with $I/\sigma > 2.0$ (14,952 reflections) stands at 17.3%. The rms deviations from ideal bond lengths and angles are 0.007 Å and 1.90°, respectively. The average B value is 35.8 Å^2 for the H-2K^b heavy chain, 40.5 Å^2 for β_2-microglobulin, 28.2 Å^2 for OVA-8, and 40.6 Å^2 for the crystallographic waters (denoted as w1–w109, corresponding to ascending B values). Luzzatti analysis (26) estimates the coordinate error to be ≈0.25 Å. PROCHECK (27) analysis shows that 91.5% of the residues reside in the most favored regions of a Ramachandran plot and that 8.2% and 0.3% (residue Asp-29) fall into additionally or generously allowed regions, respectively.

Structural Analysis. The H-2K^b–OVA-8 structure was compared with the VSV-8 and SEV-9 complexes, which have been further refined (D.H.F. and I.A.W., unpublished results) from coordinates 1VAA and 1VAB previously deposited (3) in the Protein Data Bank. Potential hydrogen bonds were calculated with the program HBPLUS (28), based upon both distance and geometric considerations. The program CONTACTSYM (29) was used to determine van der Waals (vdw) contacts of 4 Å or less. Buried surfaces were calculated with MS (30) utilizing a 1.4-Å probe sphere. Fig. 1 was made by using FRODO (23), fig. 2 and 4 were made with RIBBONS (31), and Fig. 3 and 5 were made with AVS (32).

RESULTS

OVA-8 Interactions with H-2K^b. The conformation and specific interactions of OVA-8 with H-2K^b substantiate many of the key recognition principles proposed from the comparison of the VSV-8 and SEV-9 complexes (3, 13). OVA-8 makes vdw contact with 26 residues of H-2K^b; only four of which (Glu-24, Val-76, Thr-80, and Tyr-123) do not make contact with either VSV-8 or SEV-9. Thirteen class I residues and 7 bound water molecules make a total of 22 direct hydrogen bonds to OVA-8. However, indirect hydrogen bonds (mediated by contacting water molecules and class I residues) give rise to a more extended network associated with peptide binding (Fig. 2). Of the 52 hydrogen bonds depicted in the extended network of the OVA-8 complex, 25 are conserved in the VSV-8 and SEV-9 complexes, predominantly near the N- and C-terminal pockets A and F. One significant difference is

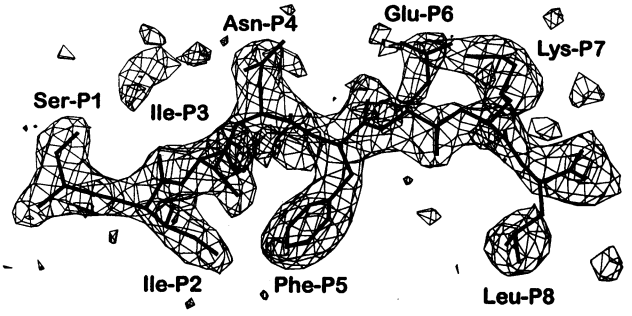

FIG. 1. F_o-F_c omit electron density map of OVA-8 (SIINFEKL) bound to H-2K^b at 2.5-Å resolution contoured at 2.5 σ.

an additional water molecule (w10) in the OVA-8 complex that supplants the role of Glu-63 by hydrogen bonding to the amide nitrogen of Ile-P2. The backbone hydrogen bonds formed with OVA-8 Asn-P4, Phe-P5, and Glu-P6 closely resemble those observed for the analogous residues of VSV-8 but not SEV-9. Three side chains of OVA-8 make hydrogen bonds directly with H-2K^b (Ser-P1 with Glu-63, Asn-P4 with Arg-155, and Lys-P7 with Ser-73), whereas only two from VSV-8 (Tyr-P3 and Gln-P6 with Glu-152) and none from SEV-9 do so.

H-2K^b Conformational Variability. Pairwise comparisons of the 27 H-2K^b residues that contact OVA-8 with the corresponding residues in the VSV-8 and SEV-9 complexes reveal that only four residues have side-chain rms deviations in excess of 1.0 Å (Lys-66, Glu-152, Arg-155, and Trp-167). The conformations of Glu-152 and Arg-155 in the OVA-8 complex are very similar to the conformations observed in the VSV-8 complex but deviate substantially from the SEV-9 complex. On the other hand, the peptide N-terminal flanking side chains of Lys-66 and Trp-167, which are similar in the VSV-8 and SEV-9 complexes, differ in the OVA-8 complex (Fig. 3). For instance, in the OVA-8 complex, Lys-66 Nζ is shifted 2.2 Å and 1.8 Å relative to the VSV-8 and SEV-9 complexes, respectively, while the position is shifted by 0.8 Å between VSV-8 and SEV-9 complexes. In all three complexes, Lys-66 Nζ hydrogen bonds with the P2 carbonyl oxygen, although this atom is shifted in the OVA-8 complex by 0.9 Å relative to both VSV-8 and SEV-9 complexes. Furthermore, in the OVA-8 complex, Lys-66 hydrogen bonds with Glu-63 Oε1 rather than Glu-63 Oε2 as in the other two complexes, which may be related to the OVA-8 Ser-P1 OH hydrogen bond with Glu-63 Oε2 and the two additional waters in the local vicinity (w10 and w30). The other significant variation is in Trp-167, which rotates inward toward the OVA-8 Ser-P1 position, with shifts in Nε1 of 1.6 Å compared to both VSV-8 and SEV-9 complexes. The analogous variation of Trp-167 was observed (6) in HLA-A2 when bound with an influenza A matrix peptide that contains a Gly at P1. Steric hindrance from either Phe-P1 or Arg-P1 would appear to prevent a similar Trp-167 conformation in the VSV-8 or SEV-9 complexes. There is one caveat, however, as Trp-167 in the OVA-8 (but not in the VSV-8 or SEV-9) complex is involved in a crystal contact; Gln-149 from a symmetry-related molecule packs within 3.7 Å of the backside of the Trp-167 indole ring. Interestingly, this may be related to the fact that the OVA-8 complex crystallizes in a different space group than VSV-8 and SEV-9 complexes ($C2$ vs. $P2_12_12$).

Buried and Exposed Peptide Residues. A total of 685 Å^2 (82.5%) of the OVA-8 solvent-accessible surface is buried in the MHC groove, whereas 829 Å^2 of H-2K^b becomes inaccessible upon peptide binding. Five side chains of OVA-8 are completely (Ile-P2, Phe-P5, and Leu-P8) or predominantly [Ser-P1 (92% inaccessible to solvent) and Ile-P3 (95%)] buried in the complex whereas only three [Asn-P4 (38%), Glu-P6 (50%), and Lys-P7 (52%)] have appreciable accessibility. OVA-8 uses the following binding pocket (13, 33) scheme:

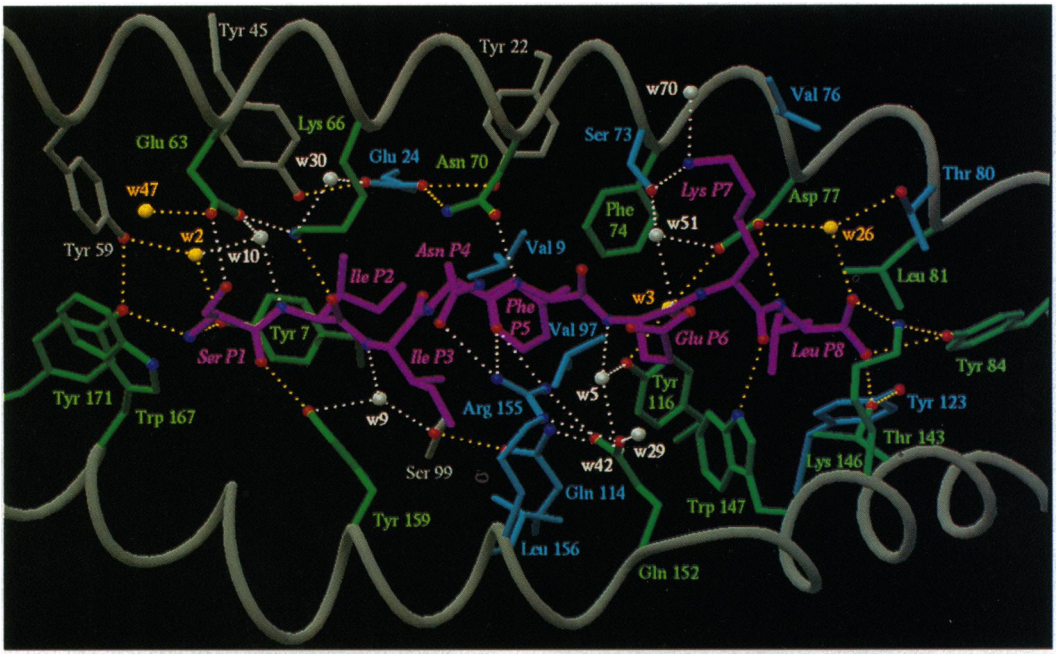

FIG. 2. Extended interactions of OVA-8 with H-2K^b. Displayed are the H-2K^b side chains that make either conserved vdw contact (green) or nonconservative vdw contact (cyan) relative to the VSV-8 and SEV-9 complexes. Conserved waters and hydrogen bonds (both direct and indirect) are yellow and nonconserved are white. Oxygens and nitrogen atoms are displayed as red and blue balls, respectively. The α1- and α2-helical segments are gray as are the four residues that, although not in vdw contact with OVA-8, nevertheless participate in the extended hydrogen bonding scheme (Tyr-22, Tyr-45, Tyr-59, and Ser-99).

Ser-P1 (pocket A), Ile-P2 (pocket B), Ile-P3 (pocket D), Phe-P5 (pocket C), and Leu-P8 (pocket F). Jameson and Bevan (34) correctly deduced the buried and accessible side chains by using Ala substitutions in the peptide sequence. In particular, they showed that, in OVA-8, Ala substitutions at positions P3, P5, and P8 reduced the stability conferred to H-2K^b on RMA-S cells, whereas replacements of P4, P6, and P7 had deleterious effects on T-cell recognition. Comparison of the exposed surfaces of the three H-2K^b complexes reveals that the chemical nature of the exposed peptide side chains is substantially different (Fig. 4). For VSV-8, both ends of the peptide are hydrophilic (Arg-P1 and Gln-P6), while the center is hydrophobic (Tyr-P3 and Val-P4). The opposite is true for SEV-9, which has hydrophobic ends (Phe-P1, Pro-P6, and Ala-P7) and a hydrophilic center (Asn-P4). In contrast, the exposed OVA-8 residues are all hydrophilic (Asn-P4, Glu-P6, and Lys-P7 with slight exposure of the Ser-P1 hydroxyl group). It seems likely that the primary level of discrimination of these complexes by T-cell receptors is at the level of the exposed peptide residues. Indeed, peptide variants of OVA-8 that are both T-cell receptor antagonists and inducers of positive selection in thymic organ culture have exposed residues that must alter the chemical and electrostatic properties of the MHC–peptide surface (Lys-P1, Glu-P1, and Arg-P4) (35).

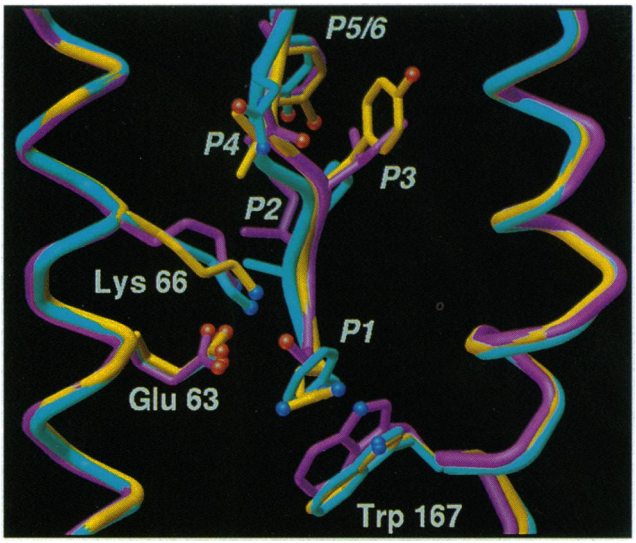

FIG. 3. OVA-8-associated conformational differences in H-2K^b. The N-terminal regions of OVA-8 (magenta), VSV-8 (yellow), and SEV-9 (cyan) complexes are rendered as tubes. The majority of MHC class I–peptide interactions are conserved in all three complexes, but nevertheless slight variations in the conformation of Glu-63, Lys-66, and especially Trp-167 are observed that apparently result from the differences in the sequences of the bound peptides.

Anchor Residue Interplay. Of particular interest is the interaction of OVA-8 Ile-P2 in the B pocket of H-2K^b with the primary anchor Phe-P5 in the C pocket (Fig. 5). In contrast to the P2 specificity pockets of products from three human class I alleles (36), the B pocket of H-2K^b is less distinct as it forms a contiguous site in conjunction with the C pocket. In both VSV-8 and SEV-9, the presence of small residues at P2 (Gly and Ala) leaves a large open cavity in the B pocket that is formed by H-2K^b residues Val-9, Glu-24, Tyr-45, and Ala-67 and into which a water molecule binds and mediates hydrogen bonding from the peptide anchor Tyr to Glu-24 and the P3 backbone (VSV-8 w57 and SEV-9 w25). In contrast, OVA-8 has a bulky Ile at P2 that packs tightly into the B pocket and is up against Phe-P5 leaving no space for water to bind because the analogous position is occupied by the Ile Cδ1 atom. Indeed, replacement of the OVA-8 anchor Phe-P5 with Tyr decreases the stability of the complex significantly (37). Likewise, an octa-Ser peptide with Ile and Phe substituted for Ser at positions P2 and P5 gives a 150-fold higher affinity than a peptide with Ile and Tyr at P2 and P5, respectively, although to attain an affinity similar to OVA-8, the Ile-P2, Phe-P5-substituted octa-Ser peptide also requires an Ile at P3 (38). Weaker binding of the Ile-P2, Tyr-P5 variant is likely for both steric and chemical reasons; the hydroxyl group would be tightly packed against the apolar Ile-P2 rather than a polar water molecule, as in VSV-8 and SEV-9. The apparent requirement of this

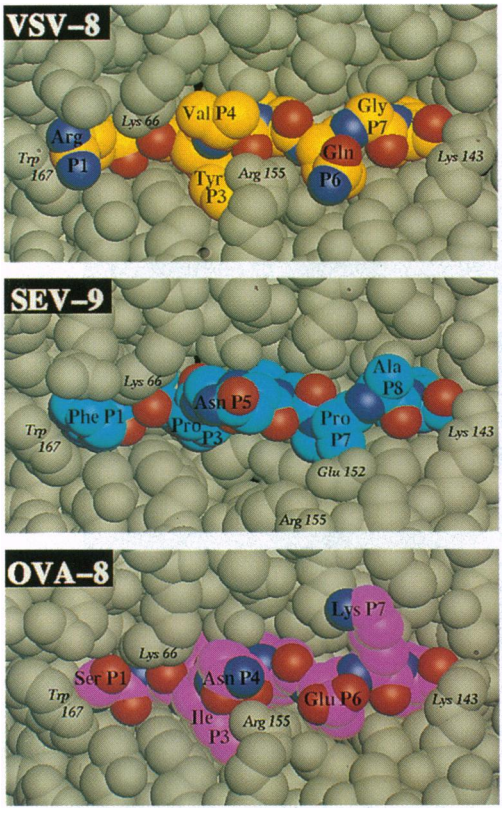

FIG. 4. Comparison of the likely T-cell contact regions of three H-2K^b complexes. Peptide contact residues of H-2K^b that exhibit significant conformational variation are labeled (Lys-66, Lys-143, Glu-152, Arg-155, and Trp-167). For all three complexes, the central residue P4 (P5 in SEV-9) has the highest accessibility to solvent; 82.5% of the surface area of OVA-8 is buried in the H-2K^b groove, compared to 82.8% of VSV-8 and 74.0% of SEV-9.

water molecule in the VSV-8 and SEV-9 complexes correlates well with the observations that (*i*) internal cavities in proteins are frequently filled with water when the potential exists for multiple hydrogen bonds (39) and (*ii*) burial of a non-

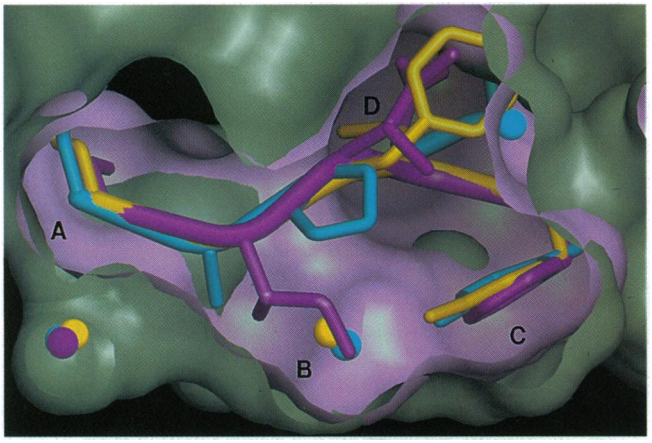

FIG. 5. Comparison of the packing of three peptides into the A–D pockets of the H-2K^b binding groove. The solvent-accessible surfaces have been calculated separately for OVA-8 (magenta) and H-2K^b (gray) in the absence of water with a clipping plane introduced to highlight the complementarity of fit. For OVA-8 (magenta), the following packing was observed: Ile-P2 in the B pocket, Ile-P3 in the D pocket, Phe-P5 in the C pocket, and the highly conserved water molecule in the A pocket. Superimposed are VSV-8 (yellow) and SEV-9 (cyan) and their contacting water molecules. In pocket B, the OVA-8 Ile-P2 Cδ1 atom appears to occupy the same space as a water molecule in the other two complexes.

hydrogen-bonded hydroxyl group in a protein interior can be energetically unfavorable (40). Thus, the Ile at the P2 position of OVA-8 is coupled to a strong preference for the smaller apolar Phe rather than Tyr as the C pocket anchor. In fact, the initially reported natural H-2K^b ligands that have the Phe-P5 anchor do indeed have an Ile at P2 (2). Preliminary peptide binding experiments with H-2K^b and a phage-display library, where individual rather than pooled sequence information is ascertained, also confirm a tight linkage of Ile-P2–Phe-P5 as one set of preferred sequences, while Ala/Gly-P2–Tyr-P5 defines a different set of high-affinity ligands (41). Exceptions to the proposed H-2K^b submotifs will no doubt be found. For instance, two natural self peptides have recently been assayed that contain Ser or Ala at P2 with Phe as the P5 anchor, albeit with lower cell surface stabilization of H-2K^b than OVA-8 (42). Both these peptides contain a Tyr at P3 that is likely to serve as a secondary anchor in a manner similar to that observed in the VSV-8 complex (i.e., filling the D pocket and hydrogen bonding with Glu-152).

DISCUSSION

In some respects the binding of peptides to MHC class I molecules is reminiscent of the packing of the core of a typical globular protein. Indeed, it appears that peptides bind with high affinity and stabilize MHC molecules by optimally complementing pockets in the core of the groove (43). The analogy is appealing for several reasons. (*i*) A significantly diverse set of sequences result in the same folded structure, although certain residues are required for optimal stability (i.e., allele-specific anchor residues). (*ii*) Preferred peptide residues can be coupled such that one residue in the packed core can influence the preferred sequence at another position (i.e., the P2 and P5 interplay in OVA-8). (*iii*) Alternate core packing can be achieved by rearrangements of side-chain torsion angles and small concerted movement of flanking secondary structure elements. (*iv*) Solvent molecules can be used to fill empty cavities and serve as hydrogen-bonding partners of buried hydrophilic residues. This comparison seems reasonable due to the conservation of the peptide conformation, the degree to which the peptide is required for stability of the class I molecule, and the extent to which the peptide is buried in the class I binding groove [70–83% for peptides bound to either human or murine alleles (3, 5, 6, 7)]. Although amino acid substitutions are easily accommodated at many peptide positions without significant loss in the stability of the complex, single substitutions of buried residues that do not significantly affect stability can apparently affect the structure of the complex, as shown by substitutions at P2 in OVA-8 that can result in differential recognition by various T-cell clones (37) or antibodies (44, 45).

Peptide-associated conformational differences have previously been identified in the structures of both H-2K^b and HLA-A2 (3, 6). Comparison of the OVA-8, VSV-8, and SEV-9 complexes with H-2K^b indicates that four side chains (Lys-66, Glu-152, Arg-155, and Trp-167) adopt peptide-specific conformations, and the study of five HLA-A2 peptide complexes identified three such residues (Arg-97, Tyr-116, and Trp-167). For both of these class I MHC molecules, a slight shift was observed in the first helical segment of the α2-helix (residues 144–151). These adjustments do not seem to be strictly correlated with peptide sequence or length (6). Further MHC–peptide structures will no doubt uncover other residues and regions that exhibit variation as a result of the binding of different peptides. Nevertheless, at present there is conflicting evidence from antibody binding data that these conformational differences are directly recognized. Hogquist *et al.* (44) used single amino acid variants of OVA-8 to investigate a panel of antibodies that had been postulated to recognize different

H-2K^b conformers but found that most of these antibodies were instead sensitive to replacements at exposed peptide residues. However, two antibodies (100.30 and 34.4.20) exhibited differential recognition of H-2K^b loaded with OVA-8 variants in which buried residues had been replaced, substitutions that may be associated with alternative conformations of the class I molecule. On the other hand, modification of the peptide structure itself may be the explanation, as there appears to be some flexibility in the way the peptide main chain lines the central portion of the binding groove (Fig. 3). Additional crystal structures of single amino acid variants of H-2K^b binding peptides would help address this issue.

The structure-based submotifs presented here for H-2K^b correlate well with existing peptide binding data. For instance, Jameson and Bevan (34) tested the six minimal-motif-containing peptides from ovalbumin in an H-2K^b stabilization assay and found OVA-8 [OVA-(257–264)] to be superior. The remaining five peptides stabilized H-2K^b in decreasing order with Val-P2–Phe-P5, Ala-P2–Phe-P5, Asn-P2–Tyr-P5, Phe-P2–Phe-P5, and Glu-P2–Tyr-P5. While other secondary anchors in the peptides could effect this ranking (i.e., P3), certain P2–P5 combinations can be predictive of strong peptide binding. What is becoming clear is that various combinations of residues can give rise to apparent high-affinity binding to class I molecules but that many of these peptides do not provide sufficient kinetic stability to enable durable survival at the cell surface. Indeed, we have found a high-affinity nonamer peptide (SRDHSRTPM) without standard anchor residues at P2, P3, and P5 that provides little thermal stabilization to H-2K^b (D.H.F., A. Brunmark, M. Jackson, P.A.P., and I.A.W., unpublished data).

We gratefully acknowledge the assistance of Yutaka Saito for protein preparations and David Jewell for discussions. This work was supported by National Institutes of Health Grants CA-58896 (I.A.W.), CA-27489 (I.A.W. and P.A.P.), CA-87489 (P.A.P.), and AI-31965 (M.M.) and Training Grant CA-09523 (D.H.F.). This is manuscript 8209-MB from The Scripps Research Institute. Coordinates of the OVA-8 complex with H-2K^b as well as the newly refined VSV-8 and SEV-9 complexes deposited in the Protein Data Bank are available (code 1VAC).

1. Germain, R. N. & Margulies, D. H. (1993) *Annu. Rev. Immunol.* **11,** 403–450.
2. Rammensee, H. G., Falk, K. & Rotzschke, O. (1993) *Annu. Rev. Immunol.* **11,** 213–244.
3. Fremont, D. H., Matsumura, M., Stura, E. A., Peterson, P. A. & Wilson, I. A. (1992) *Science* **257,** 919–927.
4. Zhang, W., Young, A. C., Imarai, M., Nathenson, S. G. & Sacchettini, J. C. (1992) *Proc. Natl. Acad. Sci. USA* **89,** 8403–8407.
5. Silver, M. L., Guo, H. C., Strominger, J. L. & Wiley, D. C. (1992) *Nature (London)* **360,** 367–369.
6. Madden, D. R., Garboczi, D. N. & Wiley, D. C. (1993) *Cell* **75,** 693–708.
7. Young, A. C., Zhang, W., Sacchettini, J. C. & Nathenson, S. G. (1994) *Cell* **76,** 39–50.
8. Ruppert, J., Sidney, J., Celis, E., Kubo, R. T., Grey, H. M. & Sette, A. (1993) *Cell* **74,** 929–937.
9. Kast, W. M., Brandt, R. M. P., Sidney, J., Drijfhout, J. W., Kubo, R. T., Grey, H. M., Melief, C. J. M. & Sette, A. (1994) *J. Immunol.* **152,** 3904–3912.
10. Huczko, E. L., Bodnar, W. M., Benjamin, D., Sakaguchi, K., Zhu, N. Z., Shabanowitz, J., Henderson, R. A., Appella, E., Hunt, D. F. & Engelhard, V. H. (1993) *J. Immunol.* **151,** 2572–2587.
11. Geluk, A., van Meijgaarden, K. E., Southwood, S., Oseroff, C., Drijfhout, J. W., de Vries, R. R. P., Ottenhoff, T. H. M. & Sette, A. (1994) *J. Immunol.* **152,** 5742–5748.
12. Falk, K., Rotzschke, O., Stevanovic, S., Jung, G. & Rammensee, H. G. (1991) *Nature (London)* **351,** 290–296.
13. Matsumura, M., Fremont, D. H., Peterson, P. A. & Wilson, I. A. (1992) *Science* **257,** 927–934.
14. Carbone, F. R. & Bevan, M. J. (1989) *J. Exp. Med.* **169,** 603–612.
15. Jackson, M. R., Song, E. S., Yang, Y. & Peterson, P. A. (1992) *Proc. Natl. Acad. Sci. USA* **89,** 12117–12121.
16. Matsumura, M., Saito, Y., Jackson, M. R., Song, E. S. & Peterson, P. A. (1992) *J. Biol. Chem.* **267,** 23589–23595.
17. Stura, E. A., Matsumura, M., Fremont, D. H., Saito, Y., Peterson, P. A. & Wilson, I. A. (1992) *J. Mol. Biol.* **228,** 975–982.
18. Matthews, B. W. (1968) *J. Mol. Biol.* **33,** 491–497.
19. Howard, A. J., Gilliland, G. L., Finzel, B. C., Poulos, T. L., Ohlendorf, D. H. & Salemme, F. R. (1987) *J. Appl. Crystallogr.* **20,** 383–387.
20. Fremont, D. H. (1993) Ph.D. dissertation (Univ. Calif., San Diego).
21. Fitzgerald, P. D. M. (1988) *J. Appl. Crystallogr.* **21,** 273–278.
22. Harada, Y., Lifchitz, A., Berthou, J. & Jolles, P. (1981) *Acta Crystallogr. Sect. A* **37,** 398–406.
23. Jones, T. A. (1978) *J. Appl. Crystallogr.* **11,** 268–272.
24. Brunger, A. T., Kuriyan, J. & Karplus, M. (1987) *Science* **235,** 458–460.
25. Engh, R. A. & Huber, R. (1991) *Acta Crystallogr. Sect. A* **47,** 392–400.
26. Luzzatti, V. (1952) *Acta Crystallogr. Sect. A* **5,** 802–810.
27. Laskowski, R. A., MacArthur, M. W., Moss, D. S. & Thornton, J. M. (1993) *J. Appl. Crystallogr.* **26,** 283–291.
28. McDonald, I. K. & Thornton, J. M. (1994) *J. Mol. Biol.* **239,** 777–793.
29. Sheriff, S., Hendrickson, W. A. & Smith, J. L. (1987) *J. Mol. Biol.* **197,** 273–296.
30. Connolly, M. L. (1983) *J. Appl. Crystallogr.* **16,** 548–558.
31. Carson, M. (1987) *J. Mol. Graphics* **5,** 103–106.
32. Upson, C., Faulhaber, T., Kamins, D., Jr., Laidlaw, D., Schlegel, D., Vroom, J., Gurwitz, R. & Van Dam, A. (1989) *IEEE Comput. Graph. Applic.* **9,** 30–42.
33. Garrett, T. P., Saper, M. A., Bjorkman, P. J., Strominger, J. L. & Wiley, D. C. (1989) *Nature (London)* **342,** 692–696.
34. Jameson, S. C. & Bevan, M. J. (1992) *Eur. J. Immunol.* **22,** 2663–2667.
35. Hogquist, K. A., Jameson, S. C., Heath, W. R., Howard, J. L., Bevan, M. J. & Carbone, F. R. (1994) *Cell* **76,** 17–27.
36. Guo, H. C., Madden, D. R., Silver, M. L., Jardetzky, T. S., Gorga, J. C., Strominger, J. L. & Wiley, D. C. (1993) *Proc. Natl. Acad. Sci. USA* **90,** 8053–8057.
37. Chen, W., McCluskey, J., Rodda, S. & Carbone, F. R. (1993) *J. Exp. Med.* **177,** 869–873.
38. Saito, Y., Peterson, P. A. & Matsumura, M. (1993) *J. Biol. Chem.* **268,** 21309–21317.
39. Rahin, A. A., Iofin, M. & Honig, B. (1986) *Biochemistry* **25,** 3619–3625.
40. Blaber, M., Lindstrom, J. D., Gassner, N., Xu, J., Heinz, D. W. & Matthews, B. W. (1993) *Biochemistry* **32,** 11363–11373.
41. Miller, J. E. W., Haaparanta, T., Brunmark, A., Castano, A. R., Jackson, M., Peterson, P. A. & Huse, W. D. (1994) *J. Cell. Biochem.* **18,** Suppl. D, 292 (abstr.).
42. Hogquist, K. A., Jameson, S. C. & Bevan, M. J. (1994) *Curr. Opin. Immunol.* **6,** 273–278.
43. Guo, H. C., Jardetzky, T. S., Garrett, T. P., Lane, W. S., Strominger, J. L. & Wiley, D. C. (1992) *Nature (London)* **360,** 364–366.
44. Hogquist, K. A., Grandea, A. G., III, & Bevan, M. J. (1993) *Eur. J. Immunol.* **23,** 3028–3036.
45. Rohren, E. M., McCormick, D. J. & Pease, L. R. (1994) *J. Immunol.* **152,** 5337–5343.